Neuron, Vol. 45, 379–388, February 3, 2005, Copyright ©2005 by Elsevier Inc. DOI 10.1016/j.neuron.2004.12.047

Voltage-Sensing Arginines in a Potassium Channel Permeate and Occlude Cation-Selective Pores

Francesco Tombola,[1] Medha M. Pathak,[2] and Ehud Y. Isacoff[1,2,*]

[1]Department of Molecular and Cell Biology and
[2]Biophysics Graduate Group
University of California, Berkeley
Berkeley, California 94720

Summary

Voltage-gated ion channels sense voltage by shuttling arginine residues located in the S4 segment across the membrane electric field. The molecular pathway for this arginine permeation is not understood, nor is the filtering mechanism that permits passage of charged arginines but excludes solution ions. We find that substituting the first S4 arginine with smaller amino acids opens a high-conductance pathway for solution cations in the Shaker K^+ channel at rest. The cationic current does not flow through the central K^+ pore and is influenced by mutation of a conserved residue in S2, suggesting that it flows through a protein pathway within the voltage-sensing domain. The current can be carried by guanidinium ions, suggesting that this is the pathway for transmembrane arginine permeation. We propose that when S4 moves it ratchets between conformations in which one arginine after another occupies and occludes to ions the narrowest part of this pathway.

Introduction

Voltage-gated ion channels play fundamental roles in cell signaling, including action potential generation, transmitter and hormone secretion, and excitation-contraction coupling (Hille, 2001). In these channels, gates located in a conserved central pore domain (consisting of segments S5, P, and S6) open and close in response to changes in membrane potential that are detected by the specialized voltage-sensing domains (VSDs) (consisting of segments S1, S2, S3, and S4) (Doyle et al., 1998; Jiang et al., 2003a). The S4 helix in each VSD has a series of positively charged amino acids (mostly arginines) spaced at intervals of three (Gandhi and Isacoff, 2002). Movement of these arginines across the membrane electric field is the core mechanism by which the channels detect changes in membrane potential (Gandhi and Isacoff, 2002; Bezanilla, 2002).

The structure of the VSDs and the nature of the movement of S4 are matters of continuing debate. In an early model, S4 was proposed to move on its own, via axial translation and/or rotation through a "canaliculus" or "gating pore," where its arginines are insulated from lipid by a polar protein environment (Goldstein, 1996; Gandhi and Isacoff, 2002). In the recent and radically different "paddle model," S4 was proposed to reside at the periphery of the channel, with the arginines in the lipid, and with S4 moving jointly with S3 (Jiang et al., 2003a, 2003b). Several studies suggest that the actual structure lies somewhere in-between these extremes and that S4 is situated at the interface between lipid and the pore domain: (1) perturbation scanning on Kv2.1 and EAG channels found both low- and high-impact faces that suggest lipid and protein interaction, respectively (Li-Smerin et al., 2000; Schonherr et al., 2002); (2) disulfide scanning on the Shaker channel indicates a close proximity of S4 to S5 (Laine et al., 2003; Gandhi et al., 2003; Neale et al., 2003; Broomand et al., 2003); and (3) recent cryo-electron microscopy in KvAP places S4 at the protein-lipid interface (Jiang et al., 2004). It remains to be determined whether the arginines of S4 interact with lipid, as proposed in the paddle model, or if they reside in a polar protein environment, as suggested by recent studies on Shaker and KvAP (Ahern and Horn, 2004; Starace and Bezanilla, 2004; Cuello et al., 2004).

We have addressed this question in the Shaker channel by making substitutions in S4 that are expected to disfavor interaction with water and favor interaction with lipid. We find that, contrary to what one would expect if S4 arginines faced lipid, substitution with smaller hydrophobic amino acids of the first S4 arginine (R1) creates a pathway for leak by monovalent cations. This current, which we refer to as the "omega current," is specific for mutations at R1 and flows through a pathway that is distinct from the central K^+ pore. Omega current is observed only when S4 is at rest and the R1 position is deep in the span of the membrane. It can be effectively carried by guanidinium, suggesting that this is the pathway through which arginine side chains normally traverse the membrane electric field. The omega current is influenced by a mutation in S2, suggesting that S2 lines the pathway. We propose that, rather than a "gating pore," in which S4 is entirely surrounded by protein, the key to voltage sensing is a guanidinium pore at the core of each VSD. Transmembrane movement of S4 carries arginines selectively through this pore. The absence of ion leak in wild-type channels suggests that S4 favors conformations where one of the arginines occupies and occludes the narrowest part of the pathway.

Results

One of the puzzles about VSD structure and motion is how to permit bulky S4 arginines to move reversibly and quickly through the membrane, while preventing ions from the intracellular and extracellular solutions from leaking through the same pathway. A leak through the VSDs would dissipate the local electric field that acts on S4, compromising voltage-sensing function, and could, if sufficiently large, lead to loss of the transmembrane ion gradient. In order to understand the basis of selective arginine permeation, we set out to examine the properties of this conduction pathway. We reasoned that if arginines cross the membrane through a specialized permeation pathway then there might be a way to make that pathway permeable to solution ions and thus both enable its characterization and shed light

*Correspondence: eisacoff@socrates.berkeley.edu

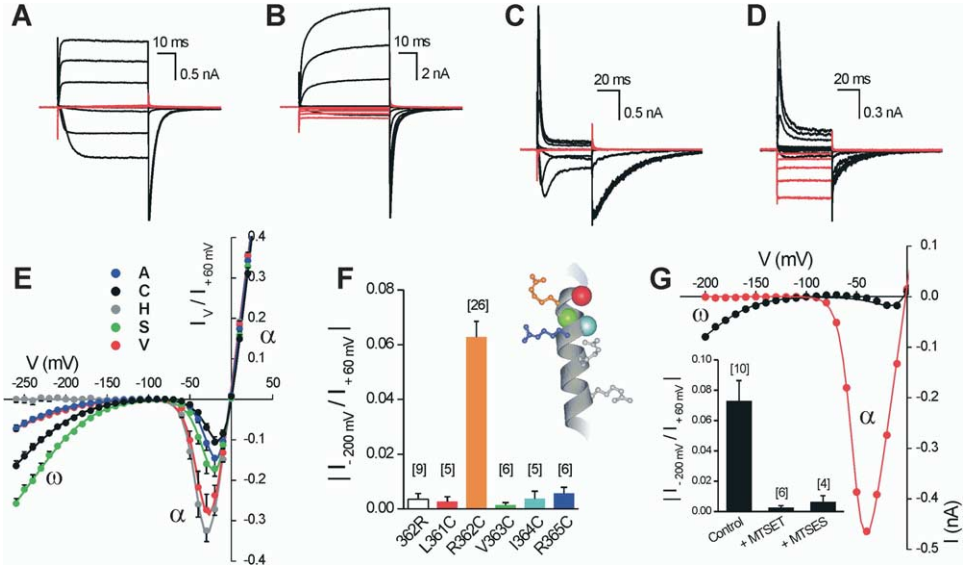

Figure 1. Substitution of Shaker R1 with Smaller Noncharged Amino Acids Brings About an Omega Current

(A–D) Representative current traces from inside-out patches of cells expressing R1 (A) or R1C (B) N-type-inactivation-removed Shaker channels and R1 (C) or R1C (D) channels with the N-terminal ball intact. R1 channels (A and C) conduct only alpha current (V > –100 mV, black traces), while R1C channels (B and D) also conduct omega current (V < –100 mV, red traces). Currents were measured while stepping from a holding potential of –110 mV to test potentials ranging from –200 to +60 mV in 20 mV steps, followed by repolarization to –80 mV (A and B) or –100 mV (C and D). Symmetrical potassium concentration yields inward alpha current at negative voltages and outward current at positive voltages (E_{rev} = 0 mV). The alpha current of R1C channels activates at more positive potentials than wild-type channels (Baker et al., 1998; Mannuzzu and Isacoff, 2000), therefore showing smaller inward alpha currents.

(E) R1A, R1C, R1S, and R1V channels conduct omega current, but R1H does not. Normalized I-V plots for the four mutants were obtained from recordings as shown in (A) and (B). Current at the end of the test pulse (I_V) normalized to current at +60 mV (see Experimental Procedures). Each point is the mean from 7 to 15 patches.

(F) Only mutations of R1 bring about omega current. Histogram reporting the normalized current at –200 mV measured in mutants compared to wild-type (first column). Number of measurements in brackets. Mutated positions are mapped on the S4 helix of the KvAP voltage sensor (inset). Side chains of arginines R1-R4 represented in ball-and-stick format.

(G) Modification of R1C by MTS reagents induces almost complete inhibition of the omega current. Representative normalized I-V plot of currents recorded from consecutive patches pulled from the same cell before (black) and after (red) treatment with [(2-trimethylammonium)-ethyl]-methanethiosulfonate (MTSET). The quantification of the inhibitions due to MTSET and to (2-sulfonatoethyl)methane-thiosulfonate (MTSES) is shown in inset.

on the mechanism by which ion leak is normally prevented.

Mutants at R1 Display an "Omega" Current

We began with mutations in the Shaker potassium channel at the first S4 arginine (Shaker residue 362, referred to as R1), because this has been recently shown to support proton conduction when replaced by a histidine (Starace and Bezanilla, 2004). We mutated R1 to alanine, cysteine, histidine, serine, and valine. In absence of a proton gradient (at pH 7.1), we found that the alanine, cysteine, serine, and valine mutants conduct a sizable inward current upon hyperpolarization (V < –100 mV) that is absent in the wild-type channel and in the histidine mutant (Figures 1A–1E). We refer to this as "omega current" to distinguish it from the typical "alpha current" that this and other voltage-gated channels conduct upon depolarization. Since channels with mutations R1C or R1S had the largest omega current, we focused on this mutation. We found that cysteine substitution at positions neighboring R1 (361, 363, 364, and 365), including R2 (365), showed no omega current (Figure 1F), indicating specificity for the R1 position. Treatment of R1C channels with both positively and negatively charged cysteine-modifying methane-thiosulfonate reagents (see Experimental Procedures for details) induced a shift to more negative potentials of the activation of the alpha current, as shown earlier (Larsson et al., 1996; Baker et al., 1998), and eliminated the omega current (Figure 1G). This confirms that the side chain of the R1 position is critical to the appearance of the omega current.

Omega Current Does Not Flow through K^+ Pore

We considered two possible explanations for the omega current. The mutations at R1 could produce an abnormal opening of the central K^+ pore, which is normally closed at negative voltage, or they could make the arginine pathway in the voltage sensor ion permeant. We tested these possibilities by examining the effect on the omega current of two different manipulations that alter the alpha current. We found that AgTx2, a polypeptide that blocks the extracellular mouth of the central K^+ pore, inhibits the alpha current (Gross and MacKinnon, 1996), but does not affect the omega current (Figures 2A and 2B). In addition, closure of the K^+

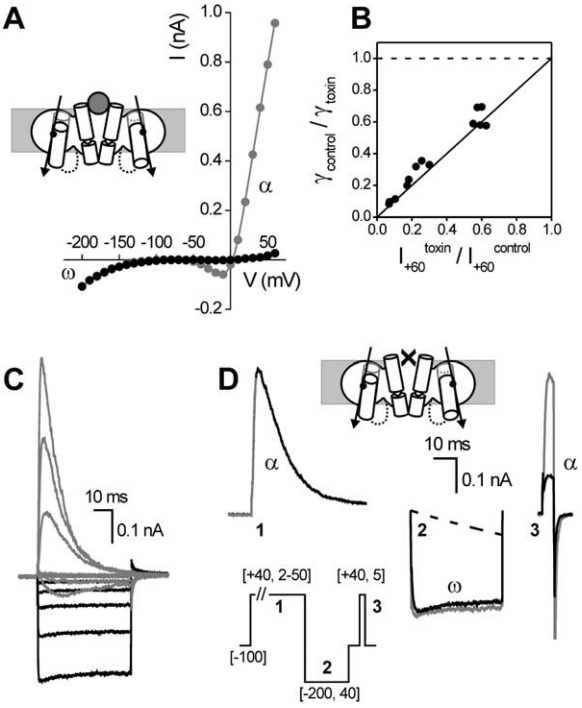

Figure 2. Block and Closure of K^+ Pore Do Not Block the Omega Current

(A) Representative I-V plots from consecutive cell-attached patch recordings from the same cell without (gray) and with (black) AgTx2 in the pipette.

(B) Comparison between the effects of AgTx2 on alpha and omega current in outside-out patches. Points are from ten experiments in which the alpha current was inhibited to different extents by AgTx2 at different concentrations. Values are $\gamma = I_{-200}/I_{+60}$. Point distribution closely follows the continuous line, representing the theoretical case of alpha current inhibition by AgTx2, with no effect on omega current (see Experimental Procedures for details).

(C and D) P-type inactivated R1C conducts omega current. (C) Current traces from an inside-out patch containing ball-deleted R1C channels with accelerated P-type inactivation (W434F/T449V, see Experimental Procedures). Currents elicited by stepping from a holding potential of –100 mV to test potentials ranging from –200 to +60 mV, in 20 mV increments. Current at V < –100 mV shown in black (omega), at V > –100 mV in gray (α). (D) Representative current traces showing effect of P-type inactivation on alpha and omega current. Omega current evoked by step to –200 mV is similar following a short (noninactivating) step (gray) and a long (inactivating) step (black), indicating that P-type inactivation closure of K^+ pore does not affect omega conductance. Potentials (in mV) and pulse lengths (in ms) indicated in brackets in voltage protocol (inset). Gray trace in step 1 (2 ms pulse) overlays black trace (50 ms pulse). Repolarization to –200 mV at end of step 1 is not shown. For clearer display, gray traces in steps 2 and 3 are shifted on the time axis to superimpose with black traces. The dashed line is the theoretical omega current if inactivated channels are *not* omega conducting. Curve generated using equation $I = I_o(1 - e^{-t/\tau})$, where I_o is the omega current in absence of inactivation and τ is the time constant for the recovery from inactivation of the alpha current estimated from the final depolarization (step 3).

pore by P-type inactivation did not alter the omega current (Figures 2C and 2D). These results indicate that the omega current flows through a pathway (which we refer to as the "omega pore") distinct from the central K^+ pore.

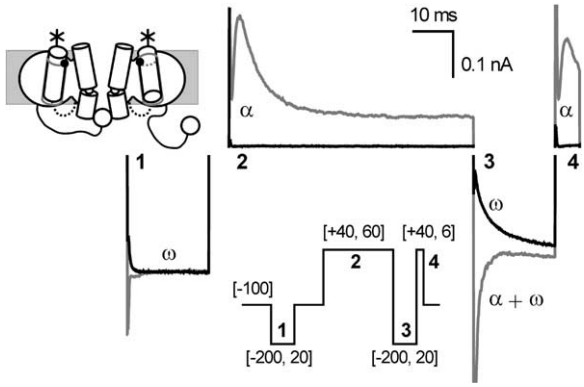

Figure 3. R1C Conducts Omega Current Only When the Voltage Sensor Is at Rest

Representative current traces from inside-out patches containing R1C with intact N-terminal inactivation ball, with (black traces) or without (gray traces) AgTx2 in the pipette. Omega current measured before (step 1) and after (step 3) a depolarization step during which the ball plugged the central pore (step 2). Potentials (in mV) and pulse lengths (in ms) are shown bracketed in inset. Omega current elicited by step 1 to –200 mV was used to normalize for the number of channels in the patch in the presence (no alpha current) and absence of AgTx2 (normal alpha current). Repolarization to –200 mV following step 2 leads to ball unbinding, followed by closure of central (alpha) pore and deactivation of the VSDs. Under normal conditions (no toxin), the central pore is transiently conducting at –200 mV when the ball detaches, and a tail of alpha current covers the rising phase of the omega current (gray trace, step 3). After suppression of the alpha current with AgTx2 in the pipette, it becomes possible to follow the kinetic of the omega current during ball detachment and to verify that the omega current rises more slowly after the depolarization step (compare black traces in steps 1 and 3). At the end of the second hyperpolarizing step the recovery from ball inactivation is not yet complete (compare peak currents in step 4 and step 2, gray traces). Accordingly, currents at the end of step 3 have not yet recovered to their original value (seen in step 1).

Omega Current in R1C Channels Requires S4 to Be at Rest

The observation that the omega current only turns on at negative voltage suggests that there may be a requirement for S4 to be in its resting conformation. To test this possibility, we exploited a specific characteristic of N-terminal ball inactivation. Opening of the internal gate of Shaker provides access for the ball to its binding site within the central K^+ pore, and once the ball is bound it prevents the gate from closing and the voltage sensor from returning to the resting conformation (Bezanilla et al., 1991). This "immobilization" lasts until the ball unbinds. We compared the onset of omega current in response to hyperpolarizing steps before and after an inactivating depolarization and found that ball inactivation significantly slows the rate at which the omega current turns on (Figure 3). The result is consistent with a requirement for S4 to be in its resting conformation. Thus, the omega current can serve as a real-time indicator of the conformational state of the VSD.

If the omega conducting state were the resting state of the VSD, then one would expect to see a correlation between the voltage dependencies of the omega cur-

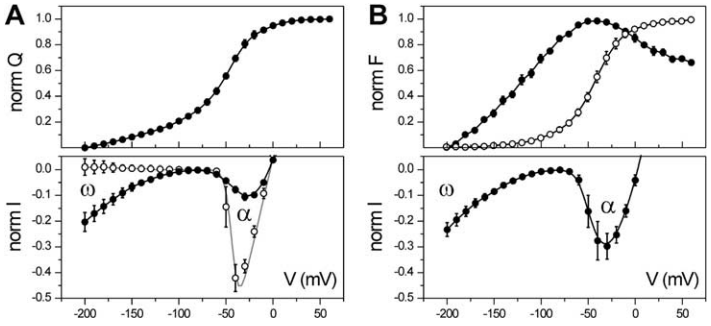

Figure 4. S4 Moves in the Voltage Range of Activation of the Omega Current

(A) Correlation between gating charge movement (upper panel) and omega pore opening (lower panel) in Shaker R1C. Normalized Q-V plot of Shaker R1C/W434F (upper panel) shows that most of the charge moves in the voltage range –100 mV to 0 mV (steep component), while a small fraction moves in the range –200 mV to –100 mV (shallow component). Gating currents were measured in TEV-clamp and the corresponding gating charges determined as reported in the Experimental Procedures (normQ = Q/Q_{max}, n = 6). Normalized I-V plot of Shaker R1C/W434 measured in TEV-clamp (lower panel, filled circles, n = 9) shows that omega pore opening occurs in the voltage range of the Q-V's shallow component (normI = I_V/I_{+60mV}). No omega current was detected in Shaker R1/W434 (open circles, n = 5).

(B) Correlation between S4 movement (upper panel) and omega pore opening (lower panel) in Shaker R1S. Normalized F-V plots of Shaker R1S/M356C/W434F (upper panel, filled circles, n = 6) and Shaker R1/M356C/W434F (open circles, n = 3) labeled with tetramethylrhodamine-5-maleimide. Fluorescence change (normF = 1 – $\Delta F/\Delta F_{max}$) is biphasic in Shaker R1S and monophasic in Shaker R1. The comparison between the two F-Vs in the voltage range –200 mV to –60 mV indicates that more-negative potentials are required to populate the resting state of Shaker R1S than those required to fully deactivate S4 in Shaker R1. I-V plot of labeled Shaker R1S/M356C/W434 (lower panel, n = 8) shows that omega pore opening occurs in the voltage range of S4 deactivation. To make the comparison between upper and lower panels easier, outward alpha currents between 0 and +60 mV are not displayed. Error bars are not shown when smaller than symbols.

rent and gating charge movement (Q-V). This is indeed what we observed. We measured the Q-V of Shaker R1C (Figure 4A, upper panel) and found that it has two components: a large component of the charge moves over the range of wild-type activation (from –100 to 0 mV) and a smaller component (~20%) moves at more negative voltages (<–100 mV). This split Q-V in R1C resembles what is seen with analogous mutations of R2 (e.g., Aggarwal and MacKinnon, 1996; Baker et al., 1998) and is consistent with a destabilization of the resting state, in which R1 and R2 are normally stabilized by electrostatic interactions within the protein (Larsson et al., 1996; Baker et al., 1998; Tiwari-Woodruff et al., 2000; Lecar et al., 2003). The small component of the Q-V likely represents the transition to and from the resting state of S4. We find that the activation of the omega current occurs in the voltage range of the small component of the Q-V (Figure 4A, lower panel), supporting the notion that the resting state of S4 is the omega conducting state.

Although the motion of S4 arginines across the electric field can account for gating charge movement (Aggarwal and MacKinnon, 1996; Seoh et al., 1996; Larsson et al., 1996; Mannuzzu et al., 1996; Yang et al., 1996; Starace et al., 1997; Starace and Bezanilla, 2004; Baker et al., 1998; Ahern and Horn, 2004), charged residues on other membrane helices could also contribute to gating charge (Seoh et al., 1996). We therefore looked for a way of determining whether S4 motion is responsible for the small component of the Q-V in the R1 mutant channel and the turn-on of the omega conductance. For this purpose, we used fluorescence to monitor S4 motion directly. To do this, we mutated R1 to serine, rather than cysteine, so that it would not be labeled with the fluorophore. The R1S channel was also engineered to contain a cysteine at position 356, which we labeled with the thiol-reactive fluorophore tetramethylrhodamine-5-maleimide (Figure 4B, upper panel). Position 356, located in the S3b-S4 loop near S4, was previously shown to be exposed to the extracellular solution both in the activated and resting states (Larsson et al., 1996) and to report on S4 movement during activation/deactivation of the VSD (Mannuzzu et al., 1996). We compared the fluorescence recordings with 356C-TMRM in Shaker R1 and in Shaker R1S. In labeled R1 channels, the largest fluorescence change was found to occur between –100 and 0 mV, the normal voltage range of activation, whereas in labeled R1S channels it occurred between –200 and –60 mV (Figure 4B, upper panel; open and filled circles, respectively), the voltage range over which the omega current turned on (Figure 4B, lower panel). The shift of the major fluorescence component to more negative potentials in R1S channels was consistent with the negative shift of a component of the Q-V measurement in R1C channels, thus indicating that more negative potentials are required to fully deactivate S4 when its first arginine is substituted with the smaller uncharged side chains. Together, the fluorescence and charge measurements are consistent with omega conductance of R1X channels turning on when S4 is in its resting position.

Ion Selectivity of Omega Current

In presence of a proton gradient, Starace and Bezanilla (2004) observed a proton current in the Shaker R1H mutant at negative voltages. In absence of proton gradient, at near neutral pH, inward proton current in R1H was too small for us to detect (Figure 1E). In contrast, in R1C the omega current at –200 mV was about 6% of the alpha current at +60 mV. This size of the current at such low proton concentration suggests that it is unlikely to be carried by protons. Indeed, we found that a 10-fold increase of the proton concentration in the pipette did not alter the omega current (data not shown). If the omega current is not carried by protons, then what ions do generate this current? We used ion substitution to try to identify these ions. Replacing chloride with the large organic anion methane-sulphonate (MES^-) in both pipette and bath solutions (see Experimental Procedures for details) did not alter the omega current (Figure 5A), indicating that the current is likely not carried by anions. The omega current was, how-

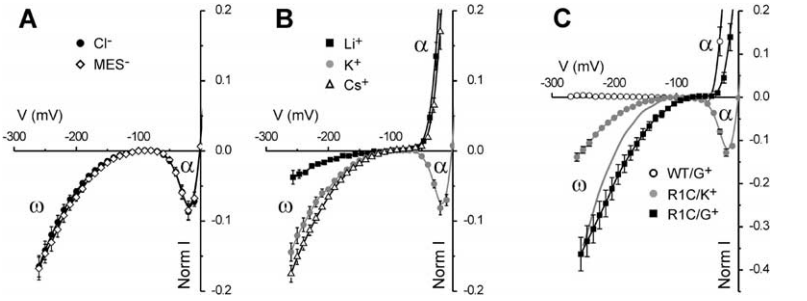

Figure 5. The Omega Pore Is Cation Selective and Conducts Guanidinium

(A) Normalized I-V plots from inside-out patches containing R1C channels. Replacement of chloride (black circles) with methanesulphonate (open diamonds) in both pipette and bath solutions does not alter the omega current (norm I = I_V/I_{+60mV}, see Experimental Procedures). Points are mean values from 8 to 11 inside-out patches.

(B) Comparison of normalized omega currents of R1C measured in inside-out patches with the pipette containing either Li^+ (black squares, n = 4–13), K^+ (gray circles, n = 9–10), or Cs^+ (open triangles, n = 10). K^+ present in the bath in all cases to provide the alpha current required for normalization (with potassium in the pipette, norm I = I_V/I_{+60mV}; with lithium, norm I = $f_{Li} \times I_V/I_{+60mV}$; with cesium, norm I = $f_{Cs} \times I_V/I_{+60mV}$; see Experimental Procedures for the meaning of f_{Li} and f_{Cs}). The omega currents carried by Cs^+ and K^+ are larger than that carried by Li^+.

(C) I-V plots of normalized omega currents from Shaker R1C carried by guanidinium (black squares, n = 11–13) and K^+ (gray circles, n = 11–12). Measurements were performed in inside-out patches with guanidinium or potassium in the pipette (when guanidinium replaces potassium in the extracellular solution, norm I = $f_{Gu} \times I_V/I_{+60mV}$; see Experimental Procedures). Gray line represents the omega current in potassium scaled to the value of the current in guanidinium at –250 mV. The omega current carried by guanidinium is larger than that carried by potassium, and its activation is shifted to less-negative potential (compare filled squares and gray line). Guanidinium does not permeate through the VSDs of wild-type Shaker channels (open circles, n = 5–7).

ever, affected by exchanging potassium with lithium or cesium in the pipette solution (Figure 5B). The order of permeation efficiency was $Cs^+ > K^+ > Li^+$. The preference for the larger cations was weak (P_{Cs}/P_K = 1.23 ± 0.11, n = 9; P_{Li}/P_K = 0.24 ± 0.05, n = 8; see Experimental Procedures) in contrast to the high selectivity of the central K^+ pore.

Our finding that substitution of an S4 arginine with smaller amino acids opened a conductance that selects against anions and has a weak selectivity between cations suggested to us that it could flow through the pathway normally taken by the arginine side chains. To examine this possibility, we asked if guanidinium ions could also carry the current. We found that guanidinium ions do carry an omega current. The guanidinium current is larger than that carried by the other cations and is not seen in oocytes expressing wild-type Shaker with its R1 intact (Figure 5C). The guanidinium omega current appears at membrane potentials less negative than those required to activate the current carried by other ions (compare filled squares and gray line in Figure 5C at V < –100 mV). As a result, the ratio between guanidinium and potassium omega currents, measured at the same voltage over the range –250 to –150 mV, increases from a value of 3.0 ± 0.5 (–250 mV, n = 11) to a value of 8.1 ± 2.4 (–150 mV, n = 12). A possible explanation for the shift in activation of the guanidinium omega current is that the occupancy of the omega pore by guanidinium stabilizes the resting conformation of Shaker R1C, so that, to reach the resting/omega-conducting conformation of the channel, less negative voltages are required.

Molecular Pathway for Omega Current

What is the environment of the R1 position that permits cations to flow at a high rate when the arginine is substituted with amino acids with small hydrophobic side chains? We examined one position, glutamate 283 in S2, because it appears to interact electrostatically with S4 arginines (Tiwari-Woodruff et al., 2000). The conservative mutation E283D produced a 6-fold increase (6.0 ± 1.1, n = 6) in the omega conductance (Figures 6A and 6B). The region around position 283 is highly accessible to the external solution in both the resting and activated states, although 283 itself is not very accessible (283C is modified by MTSET ~1000-fold more slowly than 356C, a site that is highly accessible to MTS reagents [Larsson et al., 1996; Tiwari-Woodruff et al., 2000; Gandhi et al., 2003]). This suggests that the outer end of S2 lines the external vestibule of the omega pore and that, when S4 is at rest, E283 lies near R1 in the narrow part of the omega pore.

The homologous position to E283 in EAG channels has been shown to influence the occupancy by external Mg^{2+} of a specialized S2/S3 binding site in EAG channels (Silverman et al., 2000). When bound, Mg^{2+} stabilizes the resting conformation of S4 (Schonherr et al., 2002), suggesting proximity between its binding site and S4. If Shaker had a vestibule similar to that used by Mg^{2+} to reach its binding site in EAG channels, then we would predict that Mg^{2+} would have access to the omega pore. Indeed, we found that extracellular Mg^{2+} effectively blocks the omega current (Figure 6B). Together these findings suggest that at negative voltage external cations enter a vestibule located between S2, S3 and the most N-terminal part of S4. Once in the vestibule, they can permeate into the cell if Shaker's S4 is in the resting conformation and R1 is substituted with a smaller amino acid.

The VSDs in Shaker R1C are permeable to guanidinium, but in Shaker R1 they are not ion-conducting. This could mean that, when the omega pore is occupied by the guanidino moiety of an S4 arginine, no more space is left for other ions to pass. We found that ethylguanidinium blocks the omega current carried by potassium in E283D/R1C channels (Figure 6C) while guanidinium does not (data not shown), suggesting that the omega pore is right the size to accommodate an arginine side chain but not much more.

Omega Conductance Level

We found that the ratio between the omega chord conductance of Shaker E283D/R1C measured at –270 mV

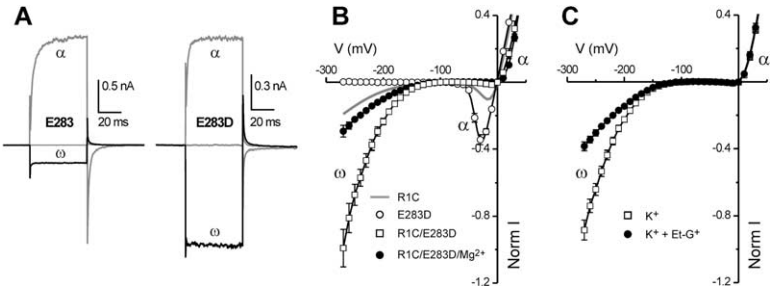

Figure 6. Properties of the Omega Pathway

(A) Mutation E283D in S2 increases the omega current of R1C channels in inside-out patches. Currents at three potentials are shown: +80, –100 (gray traces), and –260 mV (black traces). Holding potential was –100 mV. The step following the test pulse was to –60 mV for E283 and to –40 mV for E283D.

(B) Omega current is inhibited by extracellular Mg^{2+}. Normalized I-V plots of currents from patches containing E283D/R1C channels in the absence (open squares, n = 6–10) or presence of 5 mM extracellular Mg^{2+} (black circles, n = 6–11) show Mg^{2+} block of omega current. R1C (gray line) has significant omega current, but E283D (open circles, n = 10–11) does not. Note that alpha current of E283D/R1C is depolarized shifted and so shows only outward alpha current.

(C) Ethyl-guanidinium blocks the omega current carried by potassium in E283D/R1C. Normalized I-V plots from inside-out patches in the absence (open squares, n = 8–14) and presence of 10 mM extracellular ethyl-guanidinium (black circles, n = 6–7).

and the corresponding alpha chord conductance measured at +80 mV was 0.79 ± 0.09 (n = 6). If we assume a maximal open probability for the omega pore of one, a single alpha conductance of 10 pS, and if we take into account that there are four VSDs per channel, we can estimate the single VSD conductance to be ~0.6 pS. The value could be even larger, as suggested by the fact that, while the alpha chord and slope conductances are approximately the same, the omega slope conductance is about five times higher than the corresponding chord conductance ($[dI/dV]_{-270}/[G_{chord}]_{-270}$ = 4.94 ± 0.15, n = 6). In the lower estimate, the flux rate at –270 mV through a single omega pore is ~10^6 ions per second.

Discussion

The crystal structure of KvAP led to the proposal of the paddle model to describe the movement of S4 in response to voltage change (Jiang et al., 2003a, 2003b). In this model, the transmembrane movement of S4 arginines takes place within the lipid phase and no cation-conducting pore is predicted. The notion that S4 is in contact with lipid is supported by recent electron microscopy images of KvAP that show S4 to be at the channel perimeter (Jiang et al., 2004) and is consistent with the finding of a low-impact face on S4 in perturbation scanning of Kv2.1 and EAG channels (Li-Smerin et al., 2000; Schonherr et al., 2002). However, the perturbation scans both found the arginine face of S4 to be of high impact, suggesting interaction with protein. Moreover, studies on Shaker and KvAP channels have suggested that the arginine face of S4 resides in a polar environment. Residues on the arginine face of S4 have been found to be uniquely capable of carrying gating charge (Ahern and Horn, 2004), and their environment is polar enough to support a transmembrane proton flux when an arginine is substituted with histidine (Starace et al., 1997; Starace and Bezanilla, 2004), and, unlike the hydrophobic face of S4, do not appear to face lipid (Cuello et al., 2004). Does this mean that S4 arginines face a water-filled protein cavity or, given that a water wire is capable of conducting protons, could a small amount of water line the arginine face of S4 within the lipid?

Omega Pore at Core of VSD

Our observation of ionic fluxes in the order of magnitude of 10^6 metal ions per second per VSD is difficult to square with flow at the boundary of protein and lipid. This point is made more forcibly when one considers that hydrophobic substitutions at R1 would be expected to disfavor water occupancy at a lipid/protein interface, whereas we observe omega current when R1 is substituted with small hydrophobic residues and the current is eliminated by MTS conjugation that adds either a positive or negative charge to the cysteine of R1C channels. Our observations suggest that R1 faces away from lipid and into a polar protein environment. In support of this idea, we found that mutation E283D in S2 dramatically increases the omega current, consistent with proximity with R1. Together the results argue that in the resting state R1 faces into the core of the VSD, toward E283 in S2 (Figure 7).

Voltage-Sensing Motion of S4

In contrast to the resting state proximity of E283 to R1 deduced here, E283 appears to interact electrostatically with R3 and R4 in the activated state (Tiwari-Woodruff et al., 2000). In the crystal structure of the isolated VSD from the bacterial KvAP channel (Jiang et al., 2003a), R1 and R2 are exposed externally and face away from S2, while R3 and R4 are closer to the E283 homolog (KvAP D62), consistent with the activated state (Larsson et al., 1996; Mannuzzu et al., 1996; Baker et al., 1998; Wang et al., 1999; Tiwari-Woodruff et al., 2000). Earlier work suggested that the transmembrane motion of S4 consists of a combination of rotation and translation (Larsson et al., 1996; Mannuzzu et al., 1996; Yang et al., 1996; Baker et al., 1998; Cha et al., 1999; Glauner et al., 1999; Wang et al.; 1999; Tiwari-Woodruff et al., 2000; Gandhi and Isacoff, 2002; Schonherr et al., 2002; Gandhi et al., 2003, Durell et al., 2004). Our present observations can find a reasonable explanation if we consider that a helical screw motion during deactivation can move R1 into the place occupied by R4 in the isolated VSD structure (Figure 7A).

Omega Pore Occluded by a Single Arginine

Previous accessibility and mutagenesis studies on the Shaker VSDs led to the conclusion that, when S4 is at rest, R1 is the only arginine still inside the region where

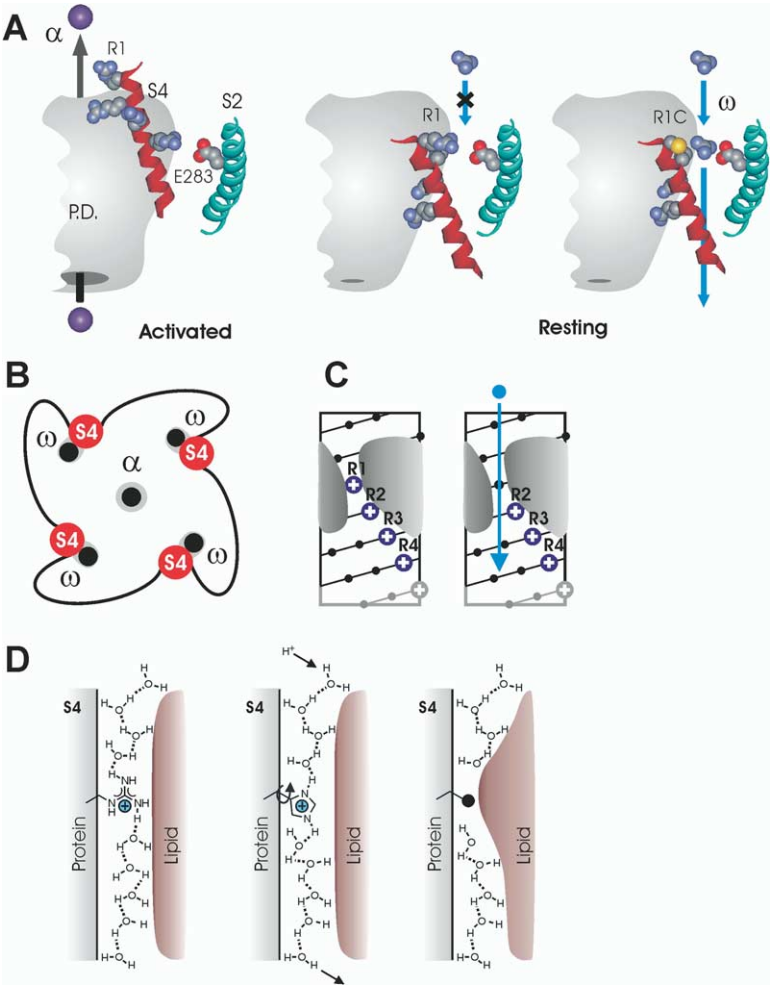

Figure 7. Proposed Location of the Omega Pore within the VSD

(A) Model of S4 and S2 lining the omega pore. The crystal structure of the isolated KvAP VSD (Jiang et al., 2003a) defines the relative positions of S2 and S4 in the activated conformation. An inward helical-screw motion of S4 ratchets R3, R2, and R1, successively, into the position occupied by R4 in the structure until R1 faces E283 in the resting state. Substitution of R1 with smaller side chains opens the pathway for ion flux at rest. The S4 helix is shown up to position G381 in Shaker (KvAP G134). Side chains displayed in space-filling CPK scheme.

(B) Likely location for the four omega pores of the Shaker channel. S4 segment is situated at subunit interface (Laine et al., 2003) and has a hydrophobic face exposed to lipid and a polar face delimiting the omega pore. This location for the S4 segments of Shaker is compatible with recent electron microscopy images of KvAP (Jiang et al., 2004). Although a clockwise orientation is illustrated, the data are equally compatible with a counterclockwise orientation.

(C) Helical net of S4 at rest illustrates how the removal of R1 can permit VSD ion conductivity.

(D) Cartoon exploring the possibility of R1 being located at the protein-lipid interface. This location could be consistent with proton conduction in the R1H VSD, but not with ion conduction through the VSD when R1 is substituted with a small hydrophobic amino acid (black sphere indicates hydrophobic side chain).

the electric field is focused (Bezanilla, 2002; Gandhi and Isacoff, 2002; Starace and Bezanilla, 2004), while R2 is at the internal edge of this region and the other arginines are exposed to the intracellular solution. It is reasonable to identify the region where the electric field is focused with the narrowest part of the arginine and omega current conduction pathway. If we consider that the substitution of R1 with a smaller amino acid is enough to let ions flow through the "arginine-conducting" omega pore and that, with S4 at rest, R2 is not inside the omega pore, we can conclude that a single arginine is sufficient to "seal" the pore. This conclusion is consistent with the finding that Shaker R2C does not conduct omega current (Figure 1F, R365C). In this mutant, when S4 is at rest, only R1 is in the omega pore, and although R2 is missing, the pore is not ion conducting. The narrowest part of the omega pore appears to be very short, suggesting a great focusing of the membrane electric field on the voltage-sensing arginines (Starace and Bezanilla, 2004).

Relationship between the Omega Pore, the R1H Proton Pore, and the Paddle Model

The concept of an omega pore occluded by R1 in wild-type Shaker and open in the R1C mutant can be made more general to include the recent finding that the VSD of Shaker R1H supports proton conduction at negative voltages (Starace and Bezanilla, 2004). In the wild-type VSD, the external and internal vestibules of the omega pore are separated by a guanidino group. Although the vestibules are expected to be filled with water molecules, protons cannot efficiently move from one vestibule to the other because the proton dissociation constant of guanidinium is too low, but they can do so when histidine replaces R1, through protonation-deprotonation cycles of the imidazole group. When a small uncharged amino acid replaces R1 there is no more physical separation between the two vestibules, and ions can pass through the open omega pore. The fact that lithium permeates the pore less efficiently than cesium or potassium and the blocking effect of magnesium on the omega current suggest that cations need to partially dehydrate to cross the narrowest part of the omega pore.

In the paddle model, where S4 arginines face lipid, there is no obvious reason why the omega current would only appear with mutations at R1 and only in the resting conformation of S4. The paddle model could potentially account for the proton current observed by Starace and Bezanilla (2004) in the R1H channel if it

were sustained by a water wire, located at the protein-lipid interface (Figure 7D), but it cannot account for the high rate of permeation by metal ions with smaller hydrophobic substitutions at R1 or for the influence of mutation at E283, which we observed here. Several pieces of evidence suggest that S4 lies at the protein-lipid interface in close proximity to the pore domain (Li-Smerin et al., 2000; Schonherr et al., 2002; Gandhi et al., 2003; Laine et al., 2003; Neale et al., 2003; Jiang et al., 2004). Our results argue that as arginines cross the membrane electric field they point away from the lipid interface and into the core of the VSD (Figures 7A and 7B), in agreement with a recent study performed on KvAP (Cuello et al., 2004) that reports evidence indicating that S4 arginines do not point toward the lipid when the channel is in a conformation similar to that corresponding to the activated state.

Arginine Permeation

The removal of the guanidino group, via substitution of R1 with smaller uncharged side chains, creates an opening through which solution ions can pass (Figures 7A–7C). In contrast to the highly selective central pore, the omega pore selects for monovalent cations but is only weakly selective between Li^+, K^+, and Cs^+. Indeed, guanidinium itself permeates the omega pore at a high rate. However, ethyl-guanidinium blocks the omega pore. This provides an indication of the size exclusion limit of the pore and supports the idea that the omega pore represents the pathway for the S4 arginines to cross the membrane.

Conclusion

We conclude that the omega pore is the nonoccluded form of the "arginine-conducting" pore in the Shaker VSD and that a single arginine side chain in the pore is sufficient to prevent flux by solution ions. We propose that the existence of a hydrophilic pathway for S4 arginines is a general feature of voltage-gated channels and that the extracellular part of this pathway could be used by external Mg^{2+} to reach its specialized binding site between S2 and S3 in EAG channels. A transmembrane motion of S4 that ratchets between resting, intermediate, and fully activated positions, as suggested by earlier work (Baker et al., 1998; Lecar et al., 2003), could ensure that most of the time one of S4's arginines is located in the narrowest part of the VSD permeation pathway, where the electric potential is expected to drop most steeply, thus optimizing the response to changes in transmembrane electric field and, at the same time, occluding the permeation pathway to prevent ion leak. The combination of lipid interaction on one hydrophobic face of S4 with a low-resistance guanidinium conducting face on the arginine side of S4 may be essential for rapid transmembrane motion of S4 and thus for the rapid reaction of voltage-gated channels to changes in membrane potential.

Experimental Procedures

Channels

Unless otherwise specified, mutations were made in the Shaker clone ShH4 Δ(6-46) (N-type inactivation removed) (Kamb et al., 1987; Hoshi et al., 1990). All point mutations were generated by PCR (Quick-Change, Stratagene) and verified by sequencing. cRNA, transcribed from HindIII-linearized DNA with T7 RNA polymerase (mMessage mMachine, Ambion), was injected in *Xenopus* oocytes (50 nl per cell, ~0.8 μg/μl). Cells were maintained at 18°C in medium (ND96) containing 96 mM NaCl, 2 mM KCl, 1.8 mM $CaCl_2$, 1 mM $MgCl_2$, 10 mM HEPES, 5 mM pyruvate, and 100 mg/L gentamycin, pH 7.2.

Electrophysiology and Voltage-Clamp Fluorometry

Patch-clamp measurements on oocytes were performed as previously described (Larsson et al., 1996) 1–3 days after injection, using an Axopatch 200A amplifier. Unless otherwise mentioned, the solution in both pipette and bath had the following composition: 100 mM KCl, 10 mM HEPES, and 1 mM EDTA, pH 7.1. In some experiments, 1 mM EDTA was replaced with 5 mM EGTA. Pipettes had initial resistance in the range 0.9–2.2 MΩ. Data were filtered at one-fifth the sampling frequency. There was no leak subtraction or compensation during recording. From the current at –100 mV, the linear leak was calculated at all potentials and subtracted offline. We verified in patches from nonexpressing oocytes that the leak had ohmic behavior in the range of the negative potentials we investigated. With guanidinium in the extracellular medium, the omega current activates at less-negative potentials than with other cations, so there is a small omega current also at –100 mV. When guanidinium replaced potassium in the pipette solution, the leak was measured at –60 mV. To obtain I-V plots normalized for the number of channels in each patch, currents at different potentials were divided by the current at +60 mV. Although the G-Vs of the mutant channels are shifted to less-negative potentials compared to the G-V of Shaker wild-type, at +60 mV all the channels are open ($P_O[\alpha]_{+60\ mV} = 1$). Shaker R1C-E283D being the only exception ($P_O[\alpha]_{+60\ mV} = 0.89 \pm 0.02$; n = 14). In the normalization procedure, we took into account that at +60 mV not all R1C-E283D α pores are open. When illustrative measurements are shown, they are representative of at least n = 4 experiments. Average values are reported ±SEM. When error bars are smaller than the symbol representing the corresponding mean value they are not shown in the plots. Modifications with MTS reagents (Toronto Research Chemicals) were carried out by perfusing the cell with bath solution containing 1 mM MTSET or MTSES for 2 min followed by extensive washing. The R1C mutation was in ShH4 Δ(6-46) with no endogenous external cysteines (mutations C245V, C462A) and with the T449V mutation to slow down P-type inactivation (Lopez-Barneo et al., 1993).

Gating currents were measured using a Dagan CA-1B amplifier (Dagan Corp., Minneapolis, MN) in two-electrode voltage-clamp mode, 7–9 days after oocyte injection. To minimize omega current interference, the composition of the recording solution was 100 mM tetraethylammonium chloride, 5 mM $MgCl_2$, and 10 mM HEPES, pH 7.5. In some cases, we used a recording solution containing 100 mM N-methyl-D-glucamine chloride, 5 mM EGTA, 5 mM $MgCl_2$, and 10 mM HEPES, pH 7.5. Gating currents were elicited by steps from –100 mV to voltages ranging from –200 to +60 mV in 10 mV increments followed by a 50 ms depolarization to +60 mV (or, alternatively, by a repolarization to –100 mV). For voltages from –200 to –120 mV, the duration of the step was 10 ms, for the remaining voltages the duration was 80 ms. No leak or linear capacitance compensation was performed during acquisition. Total transient (capacitive + gating) currents were measured in the final depolarization to +60 mV (or in the repolarization to –100 mV), integrated, and analyzed according to Aggarwal and MacKinnon (1996).

For the measurement of omega currents of Shaker R1C and R1S in two-electrode voltage-clamp, the composition of the recording solutions was 100 mM KCl, 5 mM EGTA, and 10 mM HEPES, pH 7.5. Recordings were performed the day after injection. Leak currents in two-electrode voltage-clamp did not show ohmic behavior (e.g., they were larger than linear leak at V < –100 mV) so leak subtraction was performed offline with the following procedure: cells from the same batches of those injected with RNA were injected with 90 mM KCl solution and, the day of recording, leak currents were measured from these nonexpressing cells under the same conditions used with Shaker-expressing cells (n = 5–6). Currents at voltages ranging from –200 to +60 mV were normalized for the current at –80 mV and then averaged. From the current at –80 mV in each Shaker-expressing cell, the leak was calculated at all potentials using the I-V relationship derived from mock-injected cells and subtracted from the total current.

Voltage-clamp fluorometry was performed 5–6 days after oocyte injection as previously described (Mannuzzu et al., 1996). Treatment with tetraglycine-maleimide was carried out the day of injection. A few hours before recording, cells were incubated with 5 μM tetramethylrhodamine-5-maleimide (Molecular Probes, Eugene, OR) for 20 min at 0°C and then extensively washed in ND96. After labeling, cells were kept at 10°C to slow down channel recycling at the plasma membrane. The recording solution contained 100 mM N-methyl-D-glucamine chloride, 5 mM EGTA, 5 mM $MgCl_2$, and 10 mM HEPES, pH 7.5. In some cases, 30 mM 2-mercaptoethylamine was added (and NMDG concentration reduced to 80 mM) to reduce bleaching of the fluorophore. Fluorescence changes were elicited by steps from –120 mV to voltages ranging from –200 to +60 mV in 10 mV increments (step length 20 ms). In some cases, the steps were from +60 to –200 mV. Alpha and omega currents of Shaker R1S/M356C were measured from cells subjected to the same labeling procedure used for fluorescence recordings.

Inhibition of Alpha Current

Alpha current in cell-attached and inside-out patches was inhibited by 0.8–1 μM AgTx2 (Alomone Labs) in the pipette solution, which also contained 40 μg/ml BSA (Figure 2A, black symbols, and Figure 3, black traces). In outside-out patch recordings (Figure 2B), AgTx2 was added to the bath in concentrations of 50 nM to 1 μM. BSA (30–50 μg/ml) was present in the bath before Agitoxin addition. In Figure 2B, $\gamma_{control}/\gamma_{toxin}$ ratios are plotted as a function of $I_{+60}^{toxin}/I_{+60}^{control}$ ($\gamma = I_{-200}/I_{+60}$). The continuous line represents the case of an omega current unaffected by the toxin (100% remaining omega current or 0% inhibition). Under these circumstances, $I_{-200}^{toxin} = I_{-200}^{control}$ and $I_{+60}^{toxin} = (1 - \theta) \times I_{+60}^{control}$, where θ is the fraction of blocked channels at a given Agitoxin concentration, so $(\gamma_{control}/\gamma_{toxin}) = 1 - \theta = (I_{+60}^{toxin}/I_{+60}^{control})$. If both alpha and omega current were equally inhibited by the toxin, the point distribution should follow the dashed line in Figure 2B. In that case $I_{-200}^{toxin} = (1 - \theta) \times I_{-200}^{control}$ and $I_{+60}^{toxin} = (1 - \theta) \times I_{+60}^{control}$, so $(\gamma_{control}/\gamma_{toxin}) = 1$.

Omega Current of P-Type Inactivated Channels

P-type inactivation occurs in open channels when the selectivity filter in the pore domain undergoes a conformational change that makes it nonconducting. The intracellular gate of the pore domain must close in order for the channel to recover from inactivation. Figures 2C and 2D show current traces from R1C Shaker channels that P-type inactivate during the depolarization steps. The R1C substitution was in the background of ShH4 Δ(6-46) with mutations W434F and T449V and two extracellular cysteines removed (C245V/C462A). The W434F mutation makes P-type inactivation faster than opening, and channels with this mutation do not conduct alpha current (Perozo et al., 1993). The T449V mutation, by itself, slows down P-type inactivation, so channels with both mutations have a transient alpha current with accelerated inactivation. Some authors refer to what we call P-type inactivation as either slow inactivation or C-type inactivation. The former is not specific enough and the latter is confusing because there is a separate process called C-type inactivation by Olcese et al. (1997).

Ion Permeation through Omega Pore

Since the omega current does not have a linear behavior and appears at V < –100 mV, its selectivity cannot be measured by extrapolating reversal potentials. To compare permeations of the omega pore by different ions, we compared the sizes of the normalized omega current under different ionic conditions. For the measurements in methanesulfonate, the composition of both bath and pipette solutions was 100 mM KMES, 2 mM KCl, 1 mM EDTA, and 10 mM HEPES, pH 7.1. To test lithium permeation, the pipette solution had the composition 100 mM LiCl, 2 mM KCl, 1 mM EDTA, and 10 mM HEPES, pH 7.1. To test cesium and guanidinium, LiCl was replaced by CsCl or guanidinium chloride, respectively. Applied potentials were corrected for the junction potential when needed. We measured a junction potential of –3.6 ± 0.4 mV (n = 5) with guanidinium (100 mM) in the pipette. This is in good agreement with the value –4.3 mV, calculated using a relative mobility for guanidinium $u_{Guan+}/u_{K+} = 0.68$ (D. Busath, personal communication). The omega current was normalized for the number of channels in the patch in all cases using the alpha current at +60 mV. Alpha current does not change when MES^- replaces Cl^-, but it is altered when extracellular potassium is exchanged with lithium, cesium, or guanidinium. Reducing the concentration of extracellular potassium increases the driving force for potassium outward movement, which results in an increased alpha current at +60 mV. Ionic substitution in the extracellular medium can also alter the alpha current by other means, for instance, changing the steady-state level of inactivation. To normalize for the number of channels under different ionic conditions, the current at +60 mV has to be corrected for the difference introduced by the ion exchange. We determined the correction factors for lithium and cesium in two-electrode voltage-clamp recordings on oocytes expressing Shaker R1C in which the alpha current was measured before and after exchanging extracellular potassium with lithium or cesium. The correction factors turned out to be $f_{Li} = I_{+60}(Li^+)/I_{+60}(K^+) = 1.44 \pm 0.08$ (n = 4) and $f_{Cs} = I_{+60}(Cs^+)/I_{+60}(K^+) = 1.60 \pm 0.05$ (n = 4). I-Vs in Figure 5B were corrected accordingly. For guanidinium, we determined the correction factor in outside-out patches by local extracellular perfusion of solutions containing potassium or guanidinium. The factor $f_{Gu} = I_{+60}(Guan^+)/I_{+60}(K^+) = 1.14 \pm 0.03$ (n = 7) was then used to normalize I-Vs in Figure 5C.

From the ratio between normalized omega current (I_2), measured when monovalent cations (M) other than K^+ are present in the extracellular solution, and the current (I_1), measured at the same voltage with K^+ replacing M, the permeability ratio P_M/P_K can be calculated with the simple equation

$$P_M/P_K = I_2/I_1 - 0.02 \quad (1)$$

under the experimental conditions chosen and under the assumption reported below.

If we assume independent movement of ions across the omega pore, we can write for the omega current (I) the equation

$$I = \sum_j I_j(E), \quad (2)$$

where $I_j(E)$s are the contributions of each permeating ion X_j to the total ionic current at a given transmembrane electric potential (E), and

$$I_j(E) = -z_j F \beta_j ([X_j]_{in} \exp(z_j fE) - [X_j]_{out}) / \int_{x=0}^{l} [\exp(z_j f\psi)/D_j] dx \quad (3)$$

where z_j, $[X_j]_{in}$, and $[X_j]_{out}$ are valence and intra- and extracellular concentrations of X_j, respectively. F is the Faraday's constant. β_j and D_j are the water-membrane partition coefficient and the diffusion coefficient within the membrane for X_j. ψ is the local electric potential in the membrane, $f = F/RT = 0.03934\ mV^{-1}$, and x is the depth within the membrane (see Hille, 2001).

Under the assumption that the D_js have constant values within the membrane, the omega current measured when $[K]_{out} = [K]_{in} = C_K$ and $[M]_{out} = [M]_{in} = 0$ (M = Li or Cs) is

$$I_1 = -FC_K \beta_K D_K (\exp(fE) - 1) / \int_{x=0}^{l} \exp(f\psi) dx \quad (4)$$

the omega current, measured when $[K]_{out} = A$, $[K]_{in} = C_K$, $[M]_{out} = C_M = C_K$ and $[M]_{in} = 0$, is

$$I_2 = -FC_K [\beta_K D_K (\exp(fE) - A/C_K) - \beta_M D_M] / \int_{x=0}^{l} \exp(f\psi) dx. \quad (5)$$

If the local electric potential ψ does not depend on the permeating ion, we obtain that

$$P_M/P_K = \beta_M D_M/\beta_K D_K = I_2/I_1 + (1 - I_2/I_1)\exp(fE) - A/C_K. \quad (6)$$

For $E \leq -200$ mV, $\exp(fE) \approx 0$, and for A = 2 mM and $C_K = 100$ mM, the permeability ratio becomes Equation 1. Its validity does not depend on how the local electric potential varies along the permeation pathway.

For the determination of the blocking effect of Mg^{2+} and ethyl-guanidinium on the omega current carried by potassium in Shaker R1C-E283D, we added to the pipette solution (100 mM KCl, 10 mM HEPES, and 1 mM EDTA, pH 7.1) 6 mM $MgCl_2$ (5 mM free Mg^{2+} + 1 mM MgEDTA) or 5 mM ethyl-guanidinium sulfate (10 mM free ethyl-guanidinium).

Acknowledgments

We thank P. Gorostiza for performing part of the experiments with Shaker R1S and for useful discussions and L. Kurtz and S. Wiese

for valuable technical assistance. We are grateful to R.H. Kramer for the use of his patch rig and to H. Lecar, M. Grabe, R.H. Kramer, and members of the Isacoff lab for critical comments on the manuscript. We thanks David Busath for providing the mobility of guanidinium ion. This work was supported by NIH R01NS35549 and Packard Foundation 99-8325 to E.I. and by a postdoctoral fellowship from the American Heart Association to F.T.

Received: September 12, 2004
Revised: December 15, 2004
Accepted: December 23, 2004
Published: February 2, 2005

References

Aggarwal, S.K., and MacKinnon, R. (1996). Contribution of the S4 segment to gating charge in the *Shaker* K^+ Channel. Neuron *16*, 1169–1177.

Ahern, C.A., and Horn, R. (2004). Specificity of charge-carrying residues in the voltage sensor of potassium channels. J. Gen. Physiol. *123*, 205–216.

Baker, O.S., Larsson, H.P., Mannuzzu, L.M., and Isacoff, E.Y. (1998). Three transmembrane conformations and sequence-dependent displacement of the S4 domain in shaker K+ channel gating. Neuron *20*, 1283–1294.

Bezanilla, F. (2002). Voltage sensor movements. J. Gen. Physiol. *120*, 465–473.

Bezanilla, F., Perozo, E., Papazian, D.M., and Stefani, E. (1991). Molecular basis of gating charge immobilization in Shaker potassium channels. Science *254*, 679–683.

Broomand, A., Mannikko, R., Larsson, H.P., and Elinder, F. (2003). Molecular movement of the voltage sensor in a K channel. J. Gen. Physiol. *122*, 741–748.

Cha, A., Snyder, G.E., Selvin, P.R., and Bezanilla, F. (1999). Atomic scale movement of the voltage-sensing region in a potassium channel measured via spectroscopy. Nature *402*, 809–813.

Cuello, L.G., Cortes, D.M., and Perozo, E. (2004). Molecular architecture of the KvAP voltage-dependent K^+ channel in a lipid bilayer. Science *306*, 491–495.

Doyle, D.A., Morais Cabral, J., Pfuetzner, R.A., Kuo, A., Gulbis, J.M., Cohen, S.L., Chait, B.T., and MacKinnon, R. (1998). The structure of the potassium channel: molecular basis of K+ conduction and selectivity. Science *280*, 69–77.

Durell, S.R., Shrivastava, I.H., and Guy, R.H. (2004). Models of the structure and voltage-gating mechanism of the Shaker K^+ channel. Biophys. J. *87*, 2116–2130.

Gandhi, C.S., and Isacoff, E.Y. (2002). Molecular models of voltage sensing. J. Gen. Physiol. *120*, 455–463.

Gandhi, C.S., Clark, E., Loots, E., Pralle, A., and Isacoff, E.Y. (2003). The orientation and molecular movement of a K(+) channel voltage-sensing domain. Neuron *40*, 515–525.

Glauner, K.S., Mannuzzu, L.M., Gandhi, C.S., and Isacoff, E.Y. (1999). Spectroscopic mapping of voltage sensor movement in the Shaker potassium channel. Nature *402*, 813–817.

Goldstein, S.A. (1996). A structural vignette common to voltage sensors and conduction pores: canaliculi. Neuron *16*, 717–722.

Gross, A., and MacKinnon, R. (1996). Agitoxin footprinting the Shaker potassium channel pore. Neuron *16*, 399–406.

Hille, B. (2001). Ion Channels of Excitable Membranes, Third Edition (Sunderland: Sinauer Associates).

Hoshi, T., Zagotta, W.N., and Aldrich, R.W. (1990). Biophysical and molecular mechanisms of Shaker potassium channel inactivation. Science *250*, 533–538.

Jiang, Y., Lee, A., Chen, J., Ruta, V., Cadene, M., Chait, B.T., and MacKinnon, R. (2003a). X-ray structure of a voltage-dependent K+ channel. Nature *423*, 33–41.

Jiang, Y., Ruta, V., Chen, J., Lee, A., and MacKinnon, R. (2003b). The principle of gating charge movement in a voltage-dependent K+ channel. Nature *423*, 42–48.

Jiang, Q.X., Wang, D.N., and MacKinnon, R. (2004). Electron microscopic analysis of KvAP voltage-dependent K+ channels in an open conformation. Nature *430*, 806–810.

Kamb, A., Iverson, L.E., and Tanouye, M.A. (1987). Molecular characterization of Shaker, a Drosophila gene that encodes a potassium channel. Cell *50*, 405–413.

Laine, M., Lin, M.C., Bannister, J.P., Silverman, W.R., Mock, A.F., Roux, B., and Papazian, D.M. (2003). Atomic proximity between S4 segment and pore domain in Shaker potassium channels. Neuron *39*, 467–481.

Larsson, H.P., Baker, O.S., Dhillon, D.S., and Isacoff, E.Y. (1996). Transmembrane movement of the shaker K+ channel S4. Neuron *16*, 387–397.

Lecar, H., Larsson, H.P., and Grabe, M. (2003). Electrostatic model of S4 motion in voltage-gated ion channels. Biophys. J. *85*, 2854–2864.

Li-Smerin, Y., Hackos, D.H., and Swartz, K.J. (2000). Alpha-helical structural elements within the voltage-sensing domains of a K(+) channel. J. Gen. Physiol. *115*, 33–50.

Lopez-Barneo, J., Hoshi, T., Heinemann, S.H., and Aldrich, R.W. (1993). Effects of external cations and mutations in the pore region on C-type inactivation of Shaker potassium channels. Receptors Channels *1*, 61–71.

Mannuzzu, L.M., and Isacoff, E.Y. (2000). Independence and cooperativity in rearrangements of a potassium channel voltage sensor revealed by single subunit fluorescence. J. Gen. Physiol. *115*, 257–268.

Mannuzzu, L.M., Moronne, M.M., and Isacoff, E.Y. (1996). Direct physical measure of conformational rearrangement underlying potassium channel gating. Science *271*, 213–216.

Neale, E.J., Elliott, D.J., Hunter, M., and Sivaprasadarao, A. (2003). Evidence for intersubunit interactions between S4 and S5 transmembrane segments of the Shaker potassium channel. J. Biol. Chem. *278*, 29079–29085.

Olcese, R., Latorre, R., Toro, L., Bezanilla, F., and Stefani, E. (1997). Correlation between charge movement and ionic current during slow inactivation in Shaker K^+ channels. J. Gen. Physiol. *110*, 579–589.

Perozo, E., MacKinnon, R., Bezanilla, F., and Stefani, E. (1993). Gating currents from a nonconducting mutant reveal open-closed conformations in Shaker K+ channels. Neuron *11*, 353–358.

Schonherr, R., Mannuzzu, L.M., Isacoff, E.Y., and Heinemann, S.H. (2002). Conformational switch between slow and fast gating modes: allosteric regulation of voltage sensor mobility in the EAG K+ channel. Neuron *35*, 935–949.

Seoh, S.-A., Sigg, D., Papazian, D.M., and Bezanilla, F. (1996). Voltage-Sensing residues in the S2 and S4 segments of the *Shaker* K^+ Channel. Neuron *16*, 1159–1167.

Silverman, W.R., Tang, C.Y., Mock, A.F., Huh, K.B., and Papazian, D.M. (2000). Mg(2+) modulates voltage-dependent activation in ether-a-go-go potassium channels by binding between transmembrane segments S2 and S3. J. Gen. Physiol. *116*, 663–678.

Starace, D.M., and Bezanilla, F. (2004). A proton pore in a potassium channel voltage sensor reveals a focused electric field. Nature *427*, 548–553.

Starace, D.M., Stefani, E., and Bezanilla, F. (1997). Voltage-dependent proton transport by the voltage sensor of the Shaker K+ channel. Neuron *19*, 1319–1327.

Tiwari-Woodruff, S.K., Lin, M.A., Schulteis, C.T., and Papazian, D.M. (2000). Voltage-dependent structural interactions in the Shaker K(+) channel. J. Gen. Physiol. *115*, 123–138.

Wang, M.H., Yusaf, S.P., Elliott, D.J., Wray, D., and Sivaprasadarao, A. (1999). Effect of cysteine substitutions on the topology of the S4 segment of the Shaker potassium channel: implications for molecular models of gating. J. Physiol. *521*, 315–326.

Yang, N., George, A.L., Jr., and Horn, R. (1996). Molecular basis of charge movement in voltage-gated sodium channels. Neuron *16*, 113–122.